A DATA FUSION METHOD FOR THE DELAYERING OF X-RAY FLUORESCENCE IMAGES OF PAINTED WORKS OF ART

L. D. Fiske¹, A. K. Katsaggelos¹, M. C. G. Aalders², M. Alfeld³, M. Walton¹, O. Cossairt¹

Northwestern University, Chicago II., United States
 Academic Medical Center, University of Amsterdam, Amsterdam, The Netherlands
 Delft University of Technology, Delft, The Netherlands

* LionelFiske2021@u.northwestern.edu

ABSTRACT

In this manuscript, we address the problem of studying layer structure in X-ray Fluorescence (XRF) elemental maps of paintings through the incorporation of reflectance imaging spectral data in the visible or near IR range. We propose a conceptually flexible approach, which involves an initial clustering step for the visible hyperspectral reflectance data (RIS) and the formation of a synthetic surface XRF image. Considering the difference of the full and synthetic surface XRF images, surface and subsurface correlated features are then identified. Results are demonstrated on real and simulated data.

Index Terms— XRF, RIS, Hyperspectral imaging, Data Fusion, Cultural Heritage Science

1. INTRODUCTION

Characterization of materials in the layers of painted artworks is necessary for several applications. First and foremost, these data are used to inform the preservation of the artwork. Additionally, this information can also inform studies of the artist's style and the visualization of discarded and overpainted features. Traditional approaches to this problem often involve the investigation of paint cross-sections which is damaging to the artwork. To avoid physical sampling, point analysis by a variety of chemical analytical techniques is instead employed. However, these techniques provide only local information and do not give access to information across the entire work of art. In order to acquire this sort information, imaging spectroscopy is now commonly being employed. While this addresses the aforementioned issues, the interpretation of the acquired images, especially identifying surface and subsurface features is still an open question.

Visible reflectance imaging spectroscopy (RIS) is a non-destructive and non-invasive technique in which one illumi-

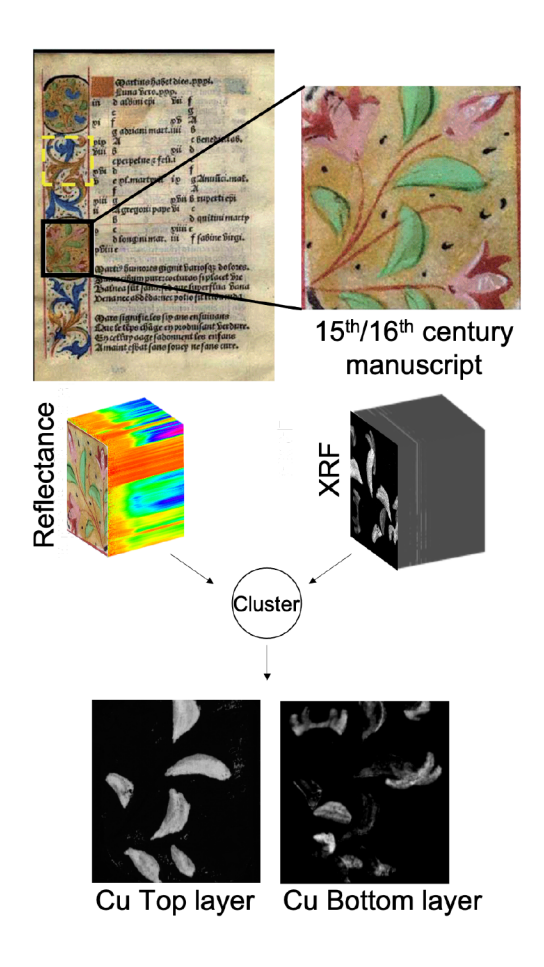


Fig. 1. Proposed framework. The input is co-registered XRF and visible reflectance (RIS) data cubes. RIS data is clustered into K pigment mixtures and the surface XRF is estimated by calculating the mean XRF response across all clusters. The subsurface XRF signal is estimated by subtracting the surface XRF from the total XRF signal.

nates an object with broadband light source and reflected light images are taken at discrete wavelengths. At each pixel, the reflectance spectrum has a characteristic shape dependent on

Funding from NSF PIRE (#1743748): Computationally-Based Imaging of Structure in Materials (CuBISM) is gratefully acknowledged. We also thank Ioanna Mantouvalou of TU Berlin (Germany) for providing us with access to the XRF strawberry data.

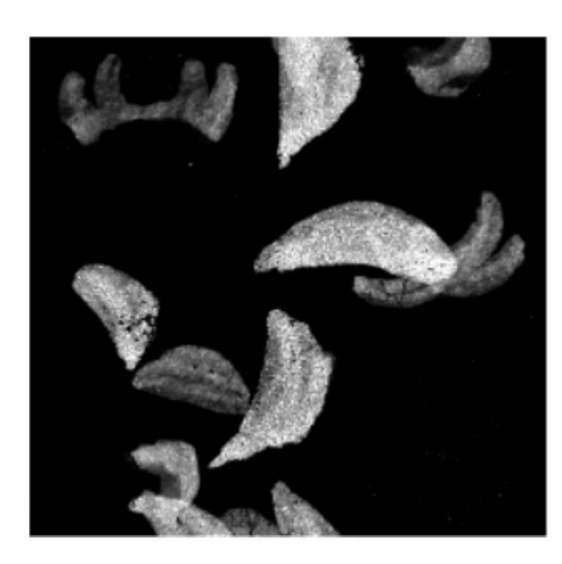


Fig. 2. Typical X-ray distribution map. Cu-Ka X-ray image showing both surface (bright pixels) and subsurface (darker pixels) features.

the material composition of the underlying pigments. In particular, many commonly used pigments have distinctive absorption features in the visible range which allow them to be unambiguously identified. However, for visible wavelength ranges up to $\sim\!800$ nm the penetration depth is relatively low. This means that virtually all of the reflected light is coming from the surface of the painting with penetration depths dependent both on the impinging wavelength and material.

Another modality routinely used for chemical imaging of works of art is X-ray fluorescence (XRF) which relies on the fact that a material excited by high energy X-rays will fluoresce at energies which are characteristic for specific elements contained in the material. By using a fitting routine, the fluorescence spectra can be mapped into a series of images where the corresponding intensity values are related to the local concentration of different atomic species [1]. An example of a Cu-K X-ray map can be seen in figure 2. Typically, XRF measurements are not depth resolved so when imaging layered structures with hidden features one observes a superposition of images as demonstrated in figures 1 and 2. While depth resolved confocal XRF can be employed to resolve features in a sublayer [2], it is a technically complex method, costly, and requires both a much higher total X-ray dose and longer acquisition times typically associated with synchrotron sources. Confocal XRF is thus not feasible for large paintings or routine applications in cultural heritage.

The key insight to this work is that light penetrates into a material structure with a depth dependant on wavelength. It is safe to assume that for visible wavelength in most paint systems, we see very little reflectance from deep buried layers. Conversely, X-rays, associated with XRF, penetrate through the entire layered structure of a painting with ease. We seek to use this diversity in penetration depths to isolate the portion

of the XRF signal which is closely associated with the surface of the painting.

2. RELATED WORK

XRF has been used in cultural heritage since the 1950s [3]. In recent years, developments in sensor technology have made XRF much more portable and accessible for Cultural heritage scientists and conservators to use [3]. XRF elemental maps can reveal hidden layers and under paintings [4] due to the penetration depth of the imaging technique. Similarly, hyperspectral imaging has become a workhorse technique for identifying surface layer pigments as well as identifying repairs [5, 6, 7].

In the field of cultural heritage science, many works of art are investigated by using both RIS and XRF. Combined RIS and XRF have been used to study the connection between stylistic changes and materiality in Late Rembrandts [8], study the composition of many illuminated manuscripts [9, 2], and to identify hidden or obscured text [10]. Currently, both techniques are being employed for the highly publicized Operation Nightwatch [11] to study and analyze materials used in the Nightwatch by Rembrandt. These modalities are also employed in other disciplines such as Geo-science, where recent work used them to study sediment cores [12]. While both RIS and XRF are often independently analyzed using quantitative techniques, the fusion of the data is typically qualitative and, with a few exceptions [7], performed by simply comparing the resulting images by eye. While some preliminary work has been done to investigate more quantitative fusion [13] this problem remains unsolved.

A similar problem has been investigated for the purpose of computationally delayering the X-radiography images [14]. In this work, a joint dictionary approach based on sparsity is employed to accomplish the separation. While the results are impressive, the problem addressed in this manuscript fundamentally differs, as all measurements are made from the surface layer of a painting. A similar one sided problem has been investigated as part of guided XRF super-resolution algorithm [15]. In this, an RGB image is used to help interpolate XRF data. This paper split the XRF signal into a portion which is correlated with the RGB and a portion which is unrelated. This splitting suffered from the fact that RGB images typically do not contain enough information for robust pigment identification because many pigment combinations are visually identical. Furthermore, a dictionary approach implicitly assumes a linear mixing model for pigments, which is nonphysical and can lead to poor results. Some newer work has used a Neural Network to find the nonlinear mapping [16] however, this approach requires information from both sides.

3. DATA SETS

To test our approach, we consider a page from a 15th/16th century Book of Tides with decoration and writing on both

sides of the page. This manuscript has been analyzed and imaged by XRF and RIS as shown in figure 1. Since by its nature, a manuscript allows easy access to the rear of the page, features on the backside can easily be compared to the results obtained through visual inspection. While having access to the rear helps with verification, will only use measurements made from a single side. Confocal XRF data was also obtained for this manuscript [2] thus providing a ground truth comparison with a different technique.

To assess the performance of the algorithm we also run it on a simulated dataset, produced from real reflectance curves for pigments clustered out of the Book of Tides dataset. We split the reflectance curves into 15 clusters and select an example cluster for red, beige, white, and green regions in figure 3 showing the ICIP logo. The respective clusters contain several hundred pixels, each with their own reflectance spectra, which we assign pixel-wise to the image. Following this, we assign each color in the image to a mean XRF response and generate a top layer XRF signal as a realization of a Poisson distribution around this mean value. Lastly, we add a simulated second image to the rear which is also realization of a Poisson random variable.

4. ALGORITHMIC DETAILS

To gain information about the XRF from the RIS, we first must map the data sets into a space where they are comparable. Conceptually, we should expect to be able to do this because a painting is made from physical materials, i.e., different paints and glazes, with a given spatial distribution and chemical structure. We expect XRF elemental map intensity and RIS data to both be functions of the physical pigment distribution. Thus, if we can successfully cluster a hyperspectral signal, such that the clusters represent the pigment concentration, we should also expect these clusters to be correlated in some way with XRF signal intensity. This is despite the fact that the reflectance signals mix in a nonlinear fashion based on the absorption and scattering properties of the pigments, fillers, and binding media [17]. Fundamentally, in this work we aim to identify portions of XRF intensity which are best related to RIS reflectance data. To do so, it is not necessary to find a physical nonlinear mapping. Instead, it is assumed that the reflectance signal $R(p_i)$ is continuous such that given 2 two mixtures of pigments p_1, p_2 , if $||R(p_1) - R(p_2)||$ is small then $||p_2 - p_1||$ is small as well. With this assumption, it is justified to cluster the reflectance data into K groups which are spectrally most similar to one another to find pixels which have the most similar surface pigment concentrations. Regions with similar surface pigment concentrations should have similar surface contributions to the XRF signal. In this work we cluster the spectra using an K-means algorithm. The example in figure 4 uses K=500. Once the initial clustering step has been performed we can make a prediction for the XRF response for each constituent cluster. Given sufficiently

large clusters, statistically independent layers, and assuming that the subsurface image is sparse, the mean XRF response should provide a sensible estimate the surface XRF signal for those pixels. We can then form an image of a predicted surface distribution by replacing each cluster of pixels in image with the mean XRF response as seen in figure 4. This allows us to estimate the surface contribution of the XRF signal as

$$\hat{X}_{surface} = \sum_{k} \mathbb{E}_{C_k} \left[X_{tot} \right] \mathbb{I}_{C_k} \tag{1}$$

Where k is the cluster index and C_k is the k_{th} cluster, and \mathbb{I}_{C_k} is the indicator function on cluster C_k . High frequency error can be introduced both by slight misregistrations as well as from hard cluster boundaries. To account for this we consider the solutions to multiple K-means clusters which have their XRF intensities slightly varied by shifting the XRF signal by single pixels relative to the reflectance cluster and different initial seeds. We estimate the surface pixel value as

$$X_{surface}^{i} = \min_{l} \left\{ \hat{X}_{surface}^{l,i} \right\} \tag{2}$$

where $\hat{X}^{l,i}_{surface}$ is the surface estimate for the i_{th} pixel given by the l^{th} clustering seed. We have found that this routine produces results with fewer errors at the boundaries than using a single estimate. The example in figure 4 uses 13 different clustering seeds and shifts. Finally, the subsurface intensity is estimated as

$$X_{subsurface}^{i} = \min(X_{tot}^{i} - X_{surface}^{i}, 0).$$
 (3)

The threshold of 0 is physically motivated from the fact that XRF elemental intensity is strictly positive.

5. RESULTS

The results on the simulated data are shown in figure 3. In this simulation it is qualitatively observed that the reconstructed surface estimate matches with the true surface XRF signal on average. Due to the fact that this is a simulation there are no uncorrelated surface effects or other sources of error so the shifting routine can be skipped. The resulting delayering is very close to the original image. You can see some residual signal remaining particularly in the regions of strong XRF signal in the green areas. The overall PSNR for the surface and subsurface is good at 24.4 and 35.9 respectively. The subsurface performance is aided in the fact that the physical threshold makes the pixel values match exactly where the image is 0.

The delayering results for the complete dataset is shown in figure 4 in which our proposed method is compared to the previously acquired confocal XRF measurements made on the same area and visible images from the front and back of the page (see [2] for complete results and conditions of acquisition). In figure 4A, the total overlapping XRF signal for the

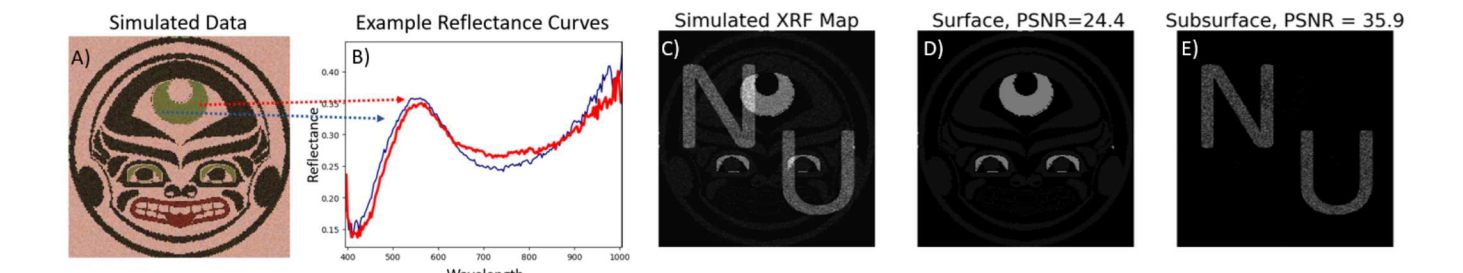


Fig. 3. We generate a simulated RIS image by reassigning pixels from the Book of Tides RIS data cube to an image of the ICIP logo and simulate an XRF by assigning each cluster a mean XRF value and adding a subsurface image. A) shows an RGB reconstruction of the simulated RIS data cube, B) examples of two green reflectance curves located at 2 different pixels. The curves have similar shapes but also contain slight differences in intensity and noise. C) shows the simulated XRF signal under Poisson noise, D) a surface XRF estimate with K=5 clusters obtained by computing the average for each cluster, E) a subsurface XRF estimate.

element Cu is observed. Our prediction for the top layer and bottom layer are shown respectively in figure 4B and C. In comparison with the previously acquired confocal XRF image of the same area (figure 4F) it is found that our result compares surprisingly well with this complex and costly method. Likewise, compared to the visible images (figures 4D and E), our algorithm may be seen to faithfully reconstruct the copper signal coming from the front and back of the page.

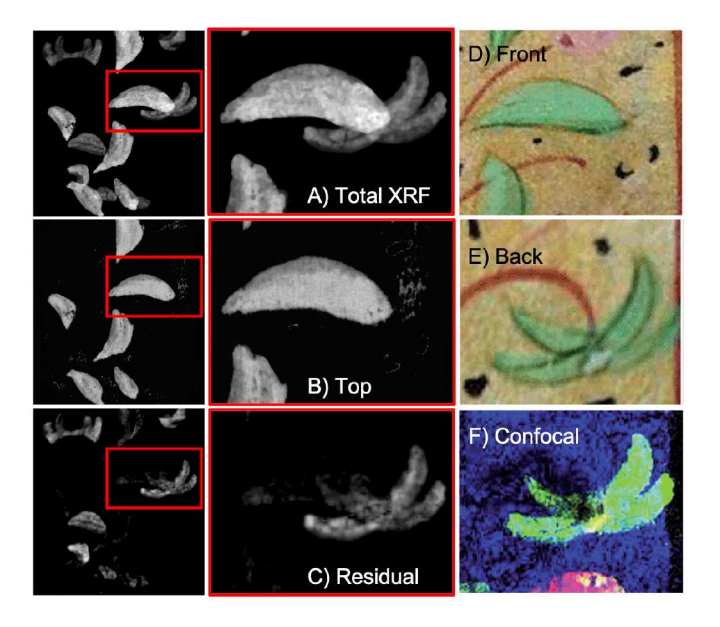


Fig. 4. Recovery of signal from an illuminated manuscript which is obscured by surface level features. A) Total Cu K XRF signal, B) estimate of Cu top layer, C) estimate of Cu bottom. D and E show visible feature of Front and Rear of manuscript. F) Cu map produced by confocal scan of same area.

6. DISCUSSION

In this paper, we discussed the problem of virtually delayering XRF elemental maps through the incorporation of RIS data. The problem of interpreting XRF data in layered media is of interest to cultural heritage scientists because it can allow for easier analysis of layering structure and the imaging of underpaintings. We proposed an approach which uses an initial clustering step and the identification of a cluster-wise response dictionary which can then be used to estimate the surface image. We demonstrated the results in simulation and on a 15th century manuscript.

Our approach is computationally simple and easy to implement and provides the end user with an easy to interpret delayering result with few parameters. This serves as an proof of concept that information of the surface XRF intensities can be gained by examining clusters in registered RIS data cubes. However, the method only can detect correlations between the XRF signal and the RIS signal so in situations where there is surface signal which is not correlated to RIS spectra the method fails. The occurs in the case of a thick layer of paint with thickness variations visible in the XRF signal. Furthermore, the method is sensitive to misregistration between the XRF and the RIS data. Which can be a difficult problem in and of itself due to contrast and resolution differences between the two measurements.

This method provides an easy to implement and effective way to estimate delayering for cultural applications involving 2 layered paintings. However, we use a very brute force clustering algorithm and ignore the underlying distributions of the XRF measurements. Several frameworks can more directly handle this sort of statistical prior such as Gaussian Mixture model or a neural network with an appropriate cost function. We intend to follow this work up by estimating the distribution of the XRF signals given for each RIS cluster and use these distributions to make inferences about layer structure.

7. REFERENCES

- [1] Matthias Alfeld and Koen Janssens, "Strategies for processing mega-pixel x-ray fluorescence hyperspectral data: a case study on a version of caravaggio's painting supper at emmaus," *J. Anal. At. Spectrom.*, vol. 30, pp. 777–789, 2015.
- [2] "Combined 1d, 2d and 3d micro-xrf techniques for the analysis of illuminated manuscripts," *J. Anal. At. Spectrom.*, no. 31, 2016.
- [3] Marco Ferretti, *X-ray Fluorescence Applications for the Study and Conservation of Cultural Heritage*, pp. 285–296, 12 2000.
- [4] Matthias Alfeld, Wout De Nolf, Simone Cagno, Karen Appel, D. Peter Siddons, Anthony Kuczewski, Koen Janssens, Joris Dik, Karen Trentelman, Marc Walton, and Andrea Sartorius, "Revealing hidden paint layers in oil paintings by means of scanning macro-xrf: a mock-up study based on rembrandt's "an old man in military costume," *J. Anal. At. Spectrom.*, vol. 40, no. 51, pp. 432–444, 2013.
- [5] Kathryn A. Dooley, Damon M. Conover, Lisha Deming Glinsman, and John K. Delaney, "Complementary standoff chemical imaging to map and identify artist materials in an early italian renaissance panel painting," *Angewandte Chemie International Edition*, vol. 53, no. 50, pp. 13775–13779, 2014.
- [6] M. Alfeld and L. de Viguerie, "Recent developments in spectroscopic imaging techniques for historical paintings - a review," *Spectrochimica Acta Part B: Atomic Spectroscopy*, vol. 136, pp. 81 – 105, 2017.
- [7] Matthias Alfeld, Silvia Pedetti, Philippe Martinez, and Philippe Walter, "Joint data treatment for vis–nir reflectance imaging spectroscopy and xrf imaging acquired in the theban necropolis in egypt by data fusion and t-sne," *Comptes Rendus Physique*, vol. 19, no. 7, pp. 625 635, 2018, Physics and arts / Physique et arts.
- [8] Kathryn A. Dooley, E. Melanie Gifford, Annelies van Loon, Petria Noble, Jason G. Zeibel, Damon M. Conover, Matthias Alfeld, Geert Van der Snickt, Stijn Legrand, Koen Janssens, Joris Dik, and John K. Delaney, "Separating two painting campaigns in saul and david, attributed to rembrandt, using macroscale reflectance and xrf imaging spectroscopies and microscale paint analysis.," Heritage Science, vol. 6, no. 46, 2018.
- [9] Aurélie Mounier and Floréal Daniel, "Hyperspectral imaging for the study of two thirteenth-century italian miniatures from the marcadé collection, treasury of the saint-andre cathedral in bordeaux, france," *Studies in Conservation*, vol. 60, no. sup1, pp. S200–S209, 2015.

- [10] E. Pouyet, S. Devine, T. Grafakos, R. Kieckhefer, J. Salvant, L. Smieska, A. Woll, A. Katsaggelos, O. Cossairt, and M. Walton, "Revealing the biography of a hidden medieval manuscript using synchrotron and conventional imaging techniques," *Analytica Chimica Acta*, vol. 982, pp. 20 30, 2017.
- [11] "Rijks museum: Operation nightwatch," Accessed: 2021-01-11.
- [12] William Rapuc, Kévin Jacq, Anne-Lise Develle, Pierre Sabatier, Bernard Fanget, Yves Perrette, Didier Coquin, Maxime Debret, Bruno Wilhelm, and Fabien Arnaud, "Xrf and hyperspectral analyses as an automatic way to detect flood events in sediment cores," *Sedimentary Geology*, vol. 409, pp. 105776, 2020.
- [13] Luis de Almeida Nieto, "XRF and RIS for semiquantitative sub-surface layer detection and composition analysis of easel paintings," M.S. thesis, TU Delft, the Netherlands, 2020.
- [14] N. Deligiannis, J. F. C. Mota, B. Cornelis, M. R. D. Rodrigues, and I. Daubechies, "X-ray image separation via coupled dictionary learning," in 2016 IEEE International Conference on Image Processing (ICIP), 2016, pp. 3533–3537.
- [15] Q. Dai, E. Pouyet, O. Cossairt, M. Walton, and A. K. Katsaggelos, "Spatial-spectral representation for x-ray fluorescence image super-resolution," *IEEE Transactions on Computational Imaging*, vol. 3, no. 3, pp. 432–444, 2017.
- [16] Wei Pu, Barak Sober, Nathan Daly, Zahra Sabet-sarvestani, Catherine Higgitt, Ingrid Daubechies, and Miguel R.D. Rodrigues, "Image separation with side information: A connected auto-encoders based approach," *Arxiv*, vol. 3, no. 3, pp. 432–444, 2017.
- [17] H. Liang, "Advances in multispectral and hyperspectral imaging for archaeology and art conservation," *Appl. Phys. A*, vol. 106, pp. 309–3230, 2012.